

## ***Supplementary Information***

### **Carbon dots/platinum nanoparticles-loaded mesoporous silica for synergistic photodynamic/catalytic therapy of hypoxic tumors**

Ke Liang,<sup>a,c</sup> Fanghao Zhao,<sup>b</sup> Fuchun Nan,<sup>a,c</sup> Jian Wang,<sup>a,c</sup> Yunxiu Zhang,<sup>a,c</sup> Jian Li,<sup>a,c</sup> Xiaokuang Xue,<sup>a,c</sup> Tiejin Chen,<sup>a,c</sup> Lin Kong,<sup>a,c</sup> Jiechao Ge,<sup>\*a,c</sup> and Pengfei Wang<sup>a,c</sup>

<sup>1</sup> Key Laboratory of Photochemical Conversion and Optoelectronic Materials and CityU-CAS Joint Laboratory of Functional Materials and Devices, Technical Institute of Physics and Chemistry, Chinese Academy of Sciences, Beijing, 100049, P. R. China

<sup>2</sup> The University of Manchester G.020 Chemistry Building, M13 9PL, Manchester, UK

<sup>3</sup> School of Future Technology, University of Chinese Academy of Sciences, Beijing, 100049, China

\*Corresponding Author E-mail: [jchge2010@mail.ipc.ac.cn](mailto:jchge2010@mail.ipc.ac.cn)

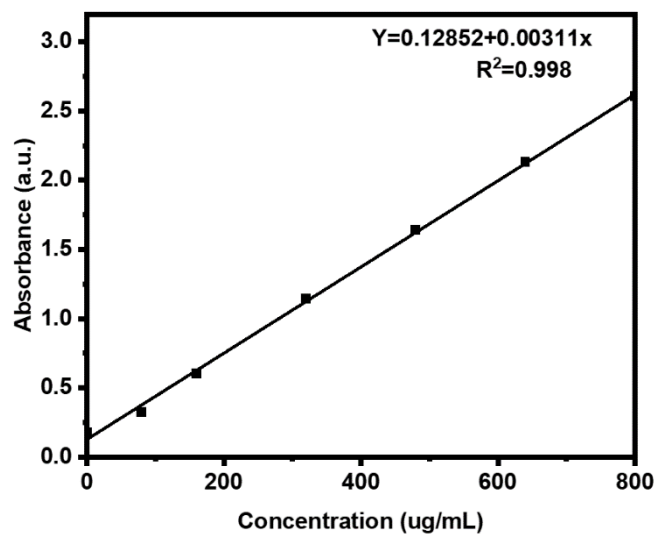


**Figure S1** Adsorption values of CDs at 485 nm under various concentrations.

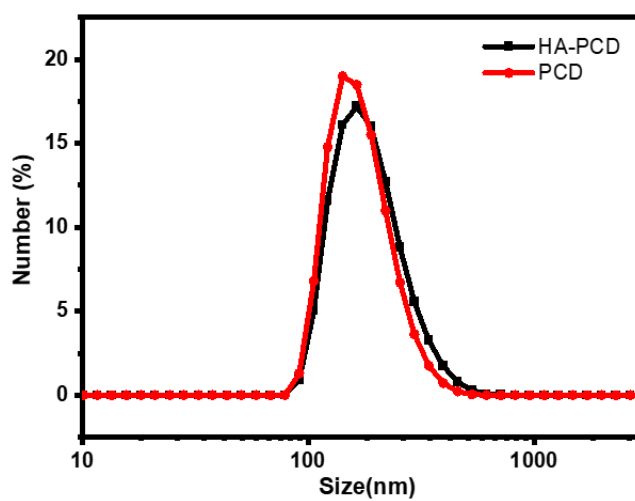


**Figure S2** DLS analysis of PCD and HA-PCD in aqueous solution.

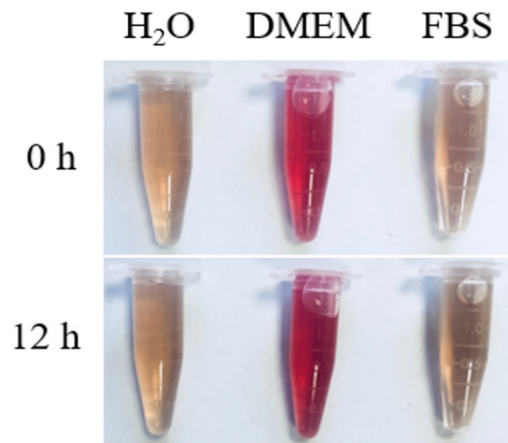


**Figure S3** The dispersed stability of HA-PCD in physiological mediums.

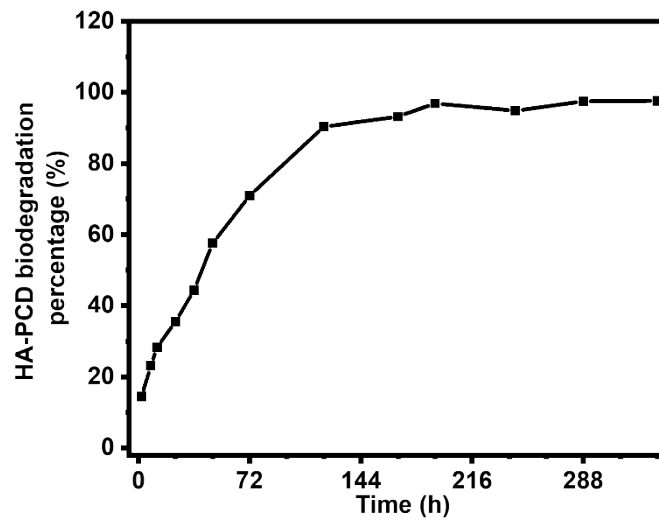


**Figure S4** The biodegradation behavior of HA-PCD in SBF.

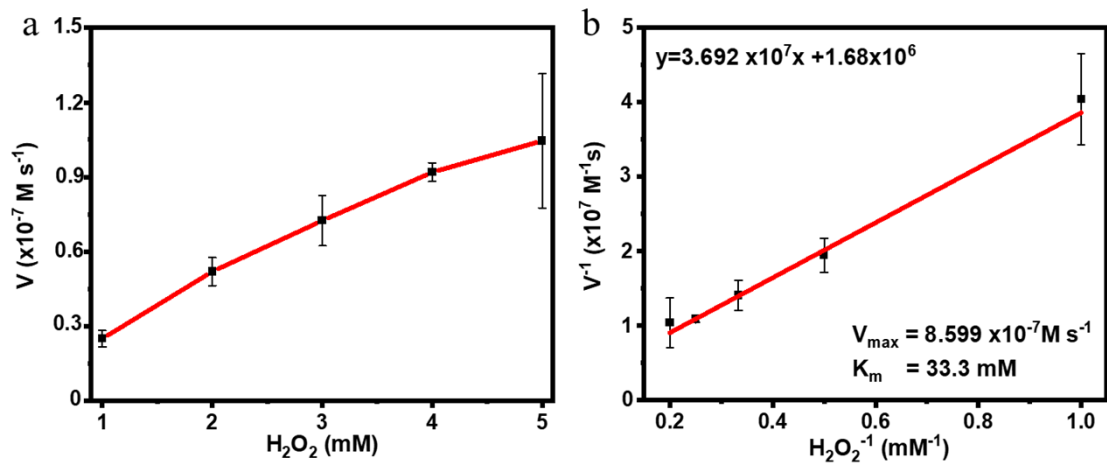


**Figure S5** (a) Michaelis-Menten kinetic analysis and (b) Lineweaver-Burk plotting for HA-PCD with  $\text{H}_2\text{O}_2$  as substrate.

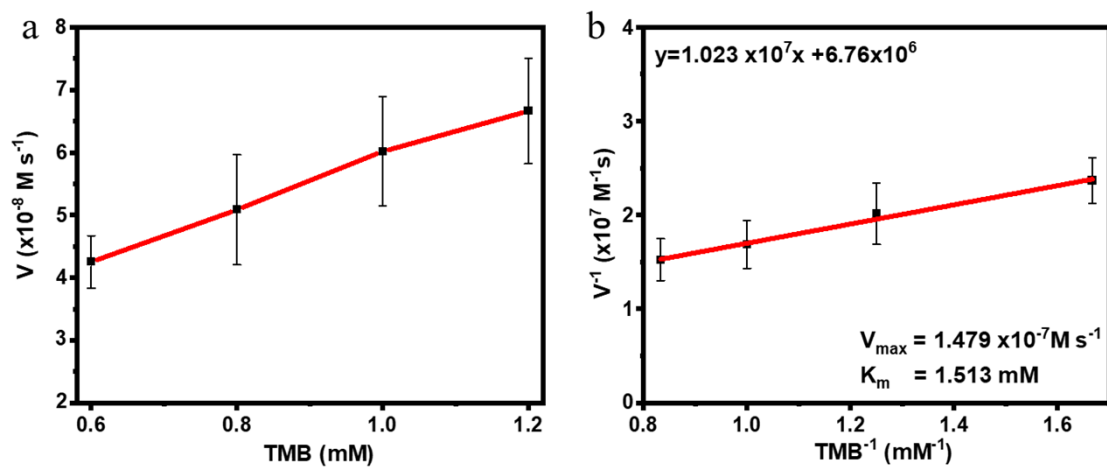


**Figure S6** (a) Michaelis-Menten kinetic analysis and (b) Lineweaver-Burk plotting for HA-PCD with TMB as substrate.

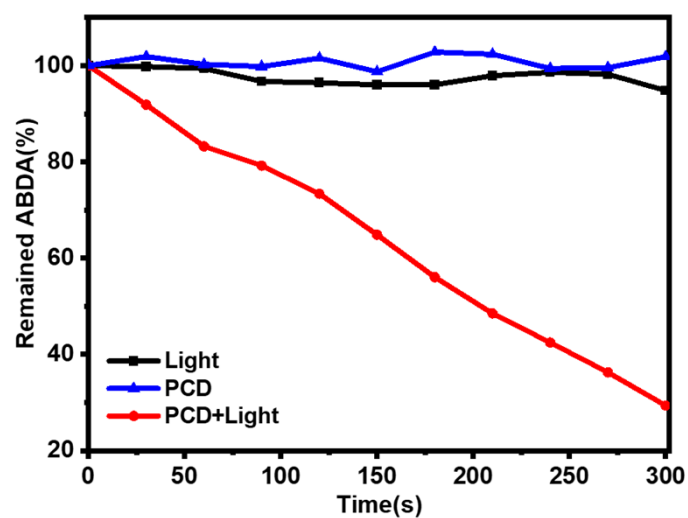


**Figure S7**  $^1\text{O}_2$  generation ability measurement of HA-PCD under normoxia condition upon 635 nm laser exposure ( $100 \text{ mW/cm}^2$ ) for various seconds, evaluated by calculating the remaining percentage of ABDA, the UV-vis absorbance at 400 nm of which would decrease in the presence of  $^1\text{O}_2$ .

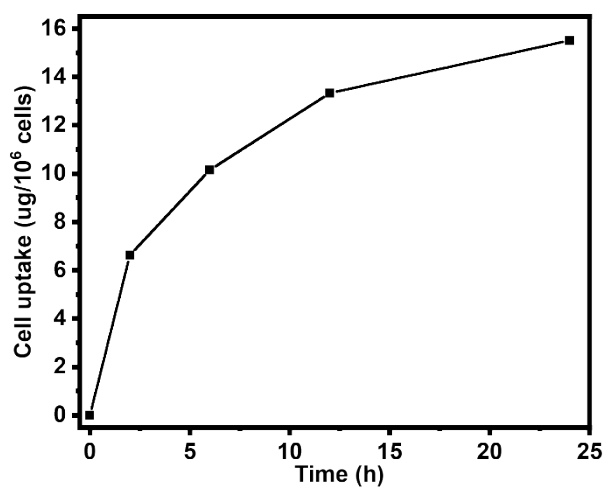


**Figure S8** The HA-PCD uptake behavior of HeLa cell at various hours.

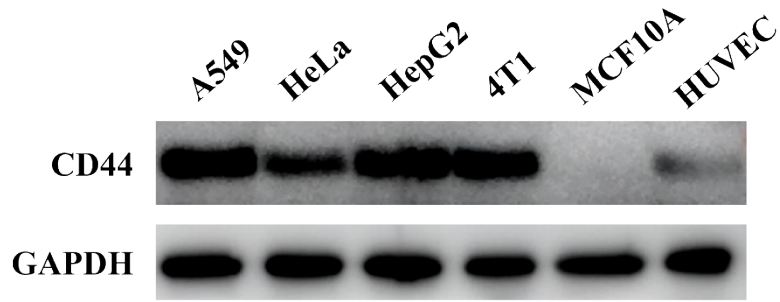


**Figure S9** Western blot analysis of the CD44 expression in A549, HeLa, HepG2, 4T1, MCF10A, and HUVEC cells.

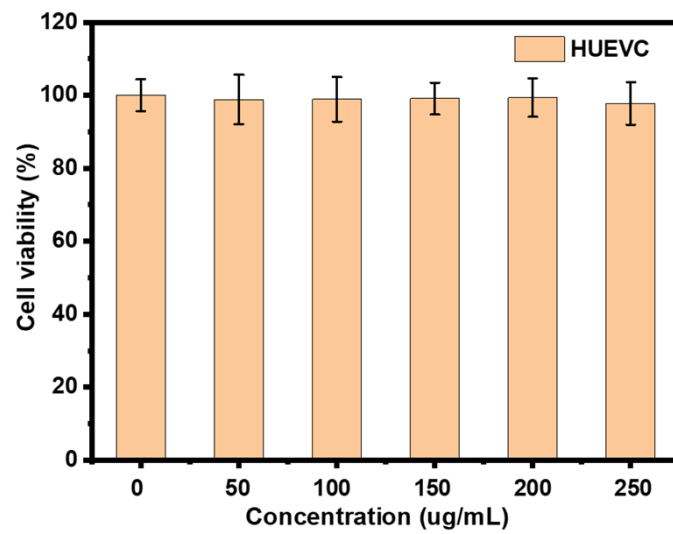


**Figure S10** Cell viability of HUVEC cells incubated with HA-PCD with different concentration.

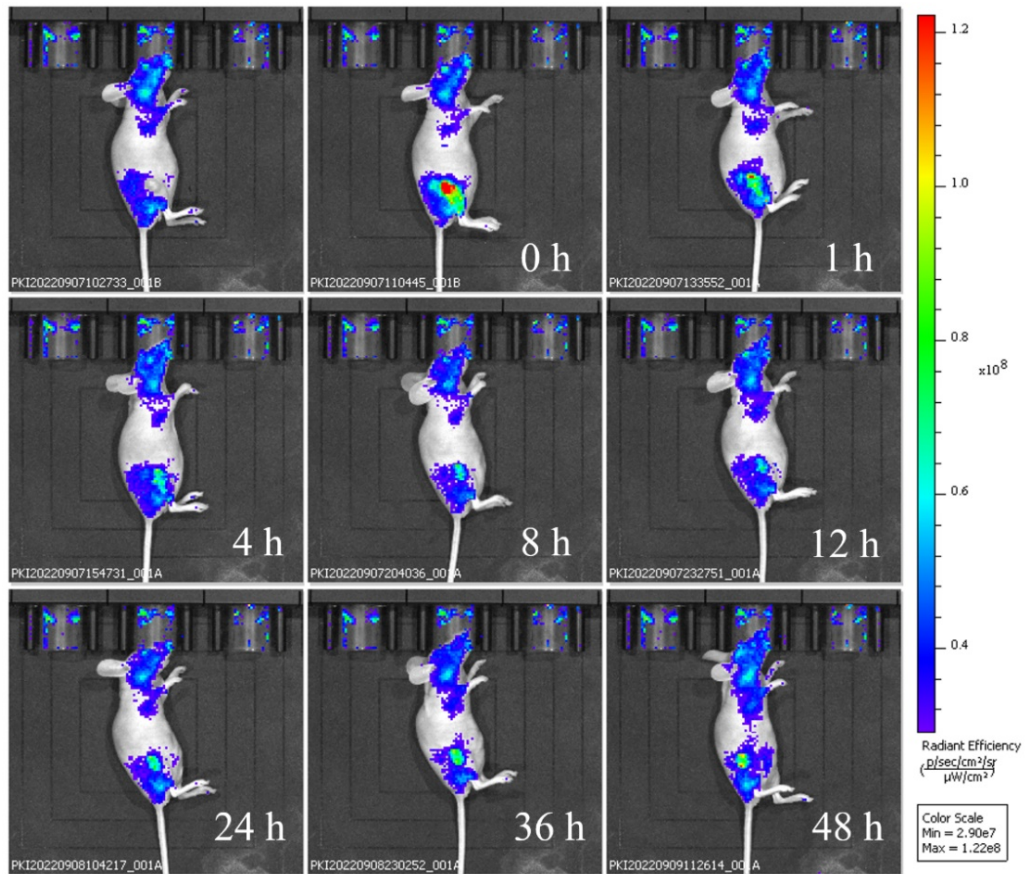
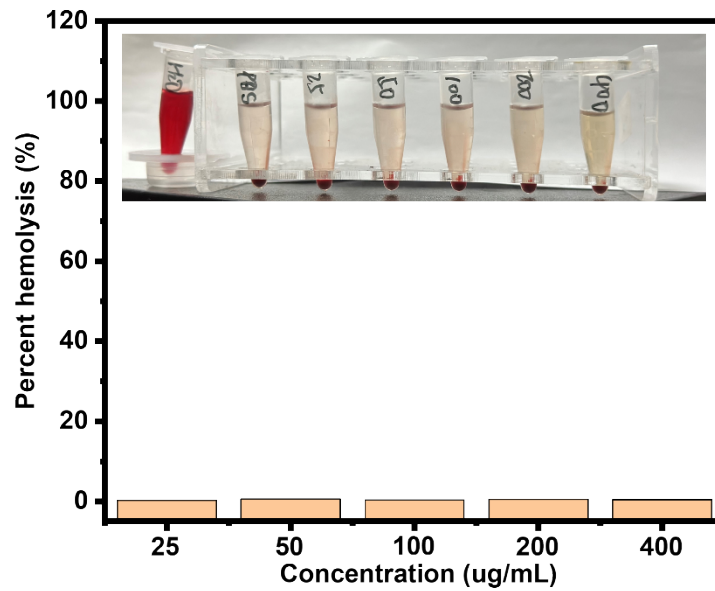


**Figure S11** FL imaging of 4T1 tumor-bearing nude mice injected with HA-PCD at



different time points.

**Figure S12** Hemolytic percent of red blood cells incubated with HA-PCD at various concentrations for 4h.





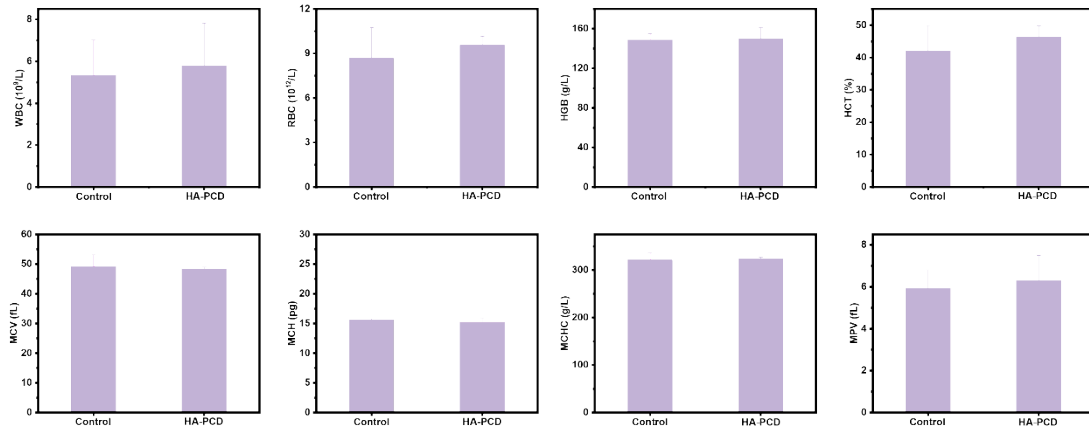


**Figure S13** Blood routine examination of the mice after injection of HA-PCD at 14d.

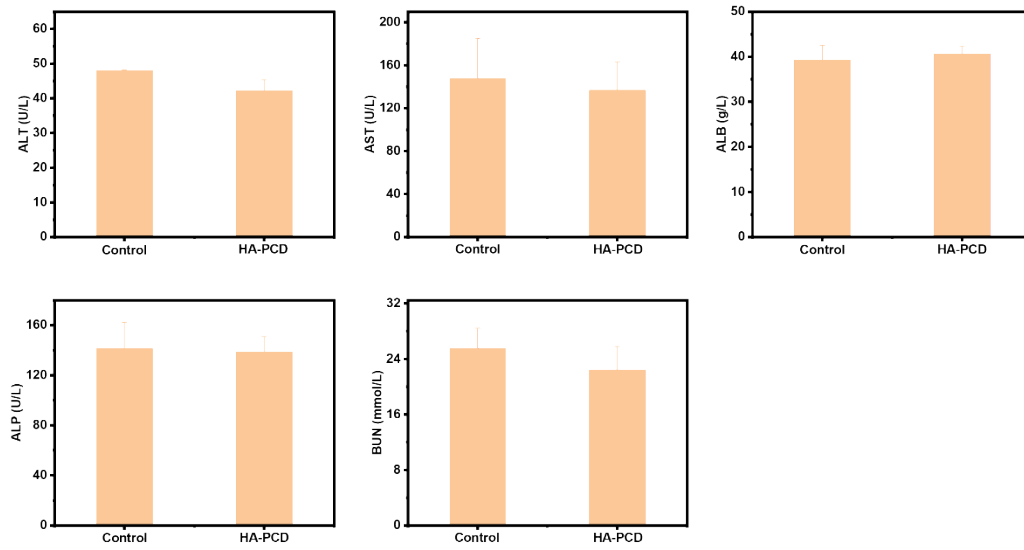


**Figure S14** Blood biochemical parameters measurement of the mice after injection of HA-PCD at 14d.

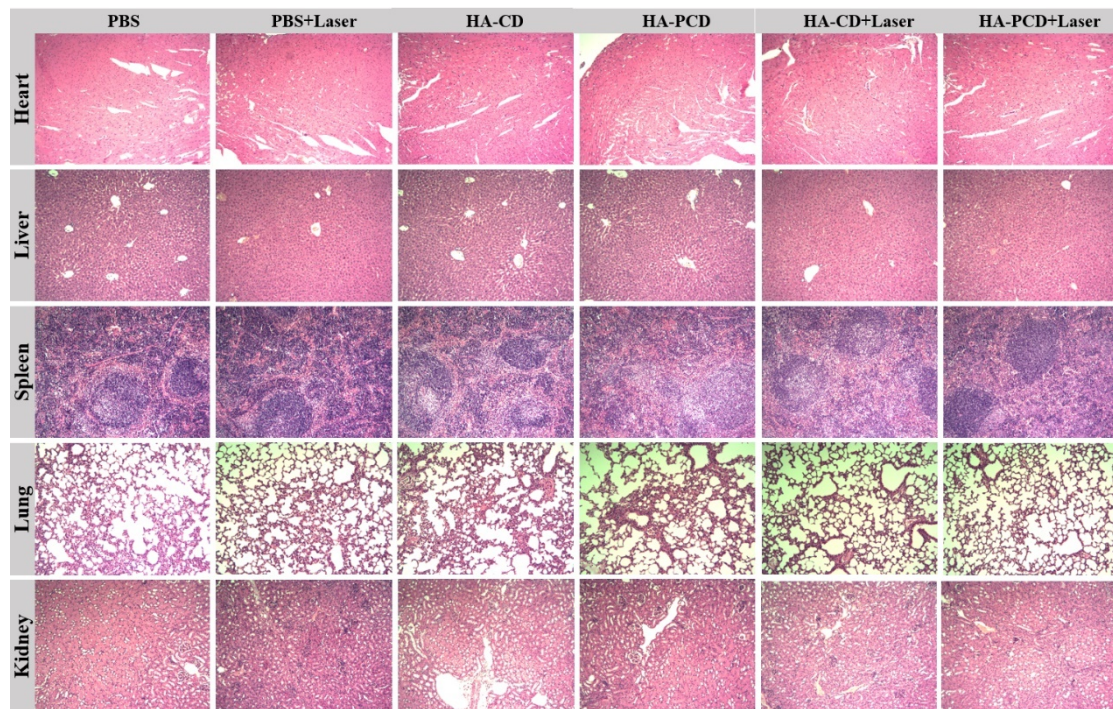


**Figure S15** H&E staining of major organs slices after different treatment.